Classification: *Biological Sciences-Neuroscience*

Dopamine synapse is a neuroligin-2-mediated contact between dopaminergic presynaptic and GABAergic postsynaptic structures

Motokazu Uchigashima[a], Toshihisa Ohtsuka[b], Kazuto Kobayashi[c], and Masahiko Watanabe[a]

[a]Department of Anatomy, Hokkaido University Graduate School of Medicine, Sapporo, Japan, [b]Department of Biochemistry, Graduate School of Medicine, University of Yamanashi, Chuo, Japan, and [c]Department of Molecular Genetics, Institute of Biomedical Sciences, Fukushima Medical University, Fukushima, Japan

Short Title: Heterologous contact at dopamine synapses

Correspondence and proofs to: **Masahiko Watanabe**, Department of Anatomy, Hokkaido University Graduate School of Medicine, Sapporo 060-8638, Japan
Fax: +81-11-706-5031; Tel: +81-11-706-5032; E-mail: watamasa@med.hokudai.ac.jp

Key words: Dopamine synapse, neuroligin-2, medium spiny neuron, striatum

Author Contributions

MU designed and performed the experiments, analyzed the data, and wrote the paper. TO and KK contributed to the data analysis. MW supervised the project and wrote the paper.

Abstract

Midbrain dopamine neurons project densely to the striatum and form so-called dopamine synapses on medium spiny neurons (MSNs), principal neurons in the striatum. As dopamine receptors are widely expressed away from dopamine synapses, it remains unclear how dopamine synapses are involved in dopaminergic transmission. Here we demonstrate that dopamine synapses are contacts formed between dopaminergic presynaptic and GABAergic postsynaptic structures. The presynaptic structure expressed tyrosine hydroxylase, vesicular monoamine transporter-2, and plasmalemmal dopamine transporter, which are essential for dopamine synthesis, vesicular filling, and recycling, but was below the detection threshold for molecules involving GABA synthesis and vesicular filling or for GABA itself. In contrast, the postsynaptic structure of dopamine synapses expressed GABAergic molecules, including postsynaptic adhesion molecule neuroligin-2, postsynaptic scaffolding molecule gephyrin, and $GABA_A$ receptor α1, without any specific clustering of dopamine receptors. Of these, neuroligin-2 promoted presynaptic differentiation in axons of midbrain dopamine neurons and striatal GABAergic neurons in culture. After neuroligin-2 knockdown in the striatum, a significant decrease of dopamine synapses coupled with a reciprocal increase of GABAergic synapses was observed on MSN dendrites. This suggests that neuroligin-2 controls striatal synapse formation by giving competitive advantage to heterologous dopamine synapses over conventional GABAergic synapses. Taking that MSN dendrites are preferential targets of dopamine synapses and express high levels of dopamine receptors, dopamine synapse formation may serve to increase the specificity and potency of dopaminergic modulation of striatal outputs by anchoring dopamine release sites to dopamine-sensing targets.

Significance Statement

Nigrostriatal dopaminergic projections form a number of dopamine synapses onto medium spiny neurons in the striatum, and have strong influence on the emotion, motivation, voluntary movement, and cognition. Despite the functional importance, the molecular composition at dopamine synapses remains unknown. Here we demonstrate that dopamine synapses are neurochemically-mismatched contacts formed between dopaminergic presynaptic and GABAergic postsynaptic structures. Intriguingly, neuroligin-2 expressed at GABAergic postsynaptic structure controls striatal synapse formation by giving competitive advantage to heterologous dopamine synapses over conventional GABAergic synapses. Therefore, our finding suggests that neuroligin-mediated formation of such neurochemically-mismatched synapses could be a novel strategy to increase the target selectivity and potency of modulation by anchoring release sites of neuromodulators to their receptive targets.

/body

Introduction

Chemical synapses comprise presynaptic machinery for transmitter release and postsynaptic machinery for receptor-mediated signal transduction in a neurochemically matched manner. They are classified into Gray type-I and type-II synapses by asymmetric or symmetric membrane density, respectively, of the pre- and postsynaptic structures (1). Most, if not all, asymmetric and symmetric synapses are excitatory and inhibitory, respectively, as they selectively express ionotropic glutamate or GABA/glycine receptors together with their specific scaffolding proteins (2). Neurochemical matching of chemical synapses is controlled by activity-dependent mechanisms (3, 4), and mediated by transmembrane adhesion proteins and secreted molecules (5). The neuroligin (NL) family comprises postsynaptic adhesion molecules that form transsynaptic contacts with presynaptic neurexins (Nrxn) (6). Of note, NL1 and NL2 are selectively expressed at glutamatergic and GABAergic synapses, respectively (7, 8) and are required for activity-dependent specification of the corresponding synapses (9).

Midbrain dopamine neurons project densely to the striatum and are strongly involved in motor and cognitive functions (10, 11). Anatomically, dopamine synapses are frequently found on dendritic shafts and spines of GABAergic medium spiny neurons (MSNs), and exhibit ultrastructural features common to symmetric synapses (12-14). MSNs constitute around 90% of all striatal neurons. They are divided equally into direct and indirect pathway MSNs (d-MSN and i-MSN), differing in their connectivity with output nuclei of the basal ganglia and in the expression of dopamine receptors, i.e., D_1R in d-MSNs and D_2R in i-MSNs (10). Considering the broad

extrasynaptic expression of D_1R and D_2R (15-17), the mode of dopaminergic transmission at dopamine synapses, i.e., whether it is mediated by *wired* transmission like that at conventional glutamatergic and GABAergic synapses, remains unclear. It is also unknown which types of molecules comprise pre- and postsynaptic membrane specializations at dopamine synapses.

In the present study, we show that the presynaptic side of dopamine synapses is indeed dopaminergic, whereas the postsynaptic side is exclusively GABAergic, expressing $GABA_A$ receptor α1 ($GABA_AR\alpha1$), gephyrin, and NL2. *In vivo* knockdown of NL2 in the striatum reduced the density of dopamine synapses on MSN dendrites, but reciprocally increased that of GABAergic synapses. Our findings suggest that NL2 regulates striatal synapse formation by giving competitive advantage to dopamine synapses over GABAergic synapses, and that the formation of dopamine synapses may serve to provide dopamine-sensing MSNs with structural anchorage of dopamine release sites.

Results

Presynaptic phenotypes at dopamine synapses

To characterize the molecular–anatomical organization of the so-called dopamine synapse, we studied the dorsolateral striatum in the adult mouse. We first examined the neurochemical properties of dopaminergic terminals, which were identified by immunolabeling for plasmalemmal dopamine transporter (DAT) or tyrosine hydroxylase (TH) (Fig. 1A and 1B). Triple immunofluorescence revealed that DAT-labeled dopaminergic terminals overlapped extensively with TH and vesicular monoamine transporter-2 (VMAT2; Fig. 1C). DAT-labeled dopaminergic terminals had no

immunodetectable signals for glutamatergic terminal markers, vesicular glutamate transporters VGluT1, VGluT2, and VGluT3, or for GABAergic terminal markers, 65/67-kDa glutamic acid decarboxylases (GAD) or vesicular inhibitory amino acid transporter (VIAAT) (Fig. S1A–S1E). However, plasmalemmal GABA transporter GAT1 was expressed in dopaminergic terminals, albeit at a much lower intensity than in VIAAT-labeled GABAergic terminals (Fig. S1F and S1G). We then compared the GABA content in dopaminergic, GABAergic, and glutamatergic terminals using immunoelectron microscopy for GABA and TH or VIAAT. According to previous studies (12, 13, 18), TH- or VIAAT-labeled terminals forming symmetric synapses were judged to be dopaminergic or GABAergic, respectively. Terminals that were unlabeled for either TH or VIAAT and formed asymmetric synapses were judged to be glutamatergic, although a few asymmetric synapses are serotonergic (19). GABAergic terminals were intensely labeled for GABA (Fig. 1D, red), whereas dopaminergic (Fig. 1E, green) and glutamatergic (Fig. 1D, blue) terminals were scarcely labeled for GABA. Density quantification revealed a significantly higher level of immunogold labeling for GABA in GABAergic terminals than in dopaminergic and glutamatergic terminals (Fig. 1F). Therefore, dopaminergic terminals contain very little, if any, GABA and GABAergic proteins, except for GAT1.

Presynaptic differentiation of dopaminergic terminals was tested by expression of the active zone protein CAST and the presynaptic adhesion molecule Nrxn. Immunofluorescence showed punctate immunolabeling for CAST in DAT-positive dopaminergic terminals (Fig. S1H). Immunoelectron microscopy revealed CAST expression beneath the presynaptic membrane of dopaminergic (Fig. 1G), GABAergic (Fig. S1I), and glutamatergic (Fig. S1J) terminals. The density of

immunogold labeling for CAST on the presynaptic membrane was comparable across the three types of terminals (Fig. 1H; open columns), and specificity was confirmed by significantly low densities of immunogold labeling in the corresponding terminals of CAST-knockout mice (Fig. 1H; filled columns). This was also true for Nrxn, which was detected at comparable levels on the presynaptic membrane of the three types of terminals (Fig. 1I, 1J, S1K, and S1L). Therefore, presynaptic molecules are recruited to the contact sites at dopaminergic terminals, like those at GABAergic and glutamatergic terminals. Together, this indicates that the presynaptic neurochemical phenotype at dopamine synapses is exclusively dopaminergic, and their contact sites exhibit presynaptic differentiation.

Dopamine receptor expression

Before investigating postsynaptic neurochemical phenotypes, we examined the basic expression profile of dopamine receptors in the striatum. Expression of D_1R and D_2R was mutually exclusive at both the transcription and protein levels (Fig. S2A and S2B), and detected predominantly along dendrites of MSNs labeled for 32 kDa dopamine- and cAMP-regulated neuronal phosphoprotein (DARPP32) (Fig. S2C). In comparison, D_1R and D_2R expression was low or undetectable in dendrites of GABAergic and cholinergic interneurons expressing their neuronal markers parvalbumin (PV), neuronal nitric oxide synthase (nNOS), and choline transporter (CHT) (Fig. S2D–S2F). In MSNs, the density of cell membrane-attached metal particles for D_1R and D_2R was comparably high in the soma, dendritic shaft, and dendritic spines (Fig. 2A–2C). In the neuropil, weak immunolabeling for D_1R and D_2R was also observed in terminals forming symmetric, but not asymmetric, synapses (Fig. 2C). Triple immunofluorescence

revealed low to moderate axonal immunolabeling for D_1R in DARPP32-positive MSN axons, and D_2R in CHT-labeled cholinergic and DAT-labeled dopaminergic axons (Fig. S2G–S2I).

Next, we examined the distribution of D_1R and D_2R in relation to dopamine synapses using double-label pre-embedding immunoelectron microscopy. Metal particles for D_1R and D_2R were densely distributed on the extrasynaptic surface of spiny dendrites, whereas the postsynaptic membrane in contact with TH-labeled dopaminergic terminals (diaminobenzidine precipitates) was rarely labeled (Fig. 2D and 2E). We quantified this by measuring the density of metal particles on the synaptic, perisynaptic (< 100 nm from the edge of the dopamine synapse), and extrasynaptic (> 100 nm) membranes (Fig. 2F). The mean labeling density for D_1R and D_2R was significantly lower in the synaptic membrane than in the extrasynaptic membrane (Fig. 2G). To test the possibility of hindered antibody penetration into dopamine synapses, we performed post-embedding immunoelectron microscopy using tissue specimens fixed mildly with 0.2% picric acid/2% paraformaldehyde fixative (Fig. S2J and S2K). Again here, the synaptic membrane of TH-labeled dopamine synapses was significantly low for D_1R or D_2R labeling than the extrasynaptic membrane (Fig. S2L and S2M). Thus, dopamine receptors are widely expressed on the extrasynaptic somatodendritic surface of MSNs, with no particular accumulation at, or gradient toward, dopamine synapses.

Postsynaptic phenotypes at dopamine synapses

We then examined which types of molecules construct postsynaptic membrane specializations at dopamine synapses. From their symmetric nature, we examined expression levels of the following GABAergic postsynaptic proteins: $GABA_AR\alpha1$,

gephyrin (a scaffolding protein interacting with $GABA_A$ and glycine receptors), and NL2 (a synaptic adhesion protein interacting with $GABA_A$ receptors and gephyrin) (20, 21). All three proteins were clustered in the neuropil, and tightly apposed to VIAAT-labeled GABAergic (Fig. 3A–3C, arrowheads) and DAT-labeled dopaminergic (arrows) terminals. Postsynaptic localization of these proteins was further tested by post-embedding double-label immunoelectron microscopy (Fig. 3D–3F and S3A–S3C). The density of immunogold labeling for $GABA_A R\alpha 1$, gephyrin, and NL2 was almost comparable between dopamine and GABAergic synapses, whereas the density at glutamatergic synapses was not different from background (Fig. 3G–3I). In contrast, glutamatergic postsynaptic proteins, PSD-95 and AMPA receptors, were enriched at glutamatergic synapses, but hardly detected at dopamine or GABAergic synapses (Fig. S3D–S3G). Therefore, the postsynaptic phenotype at dopamine synapses is exclusively GABAergic.

Postsynaptic target of dopamine synapses

Dopamine synapses are frequently found in dendritic shafts and spines of MSNs (12, 13). In the present study, we quantitatively assessed target striatal neurons by lentivirus-mediated single neuronal labeling with green fluorescence protein (GFP) (Fig. S4A and S4B). GFP-labeled dendrites (green) were further examined by immunofluorescence for TH (blue), NL2 (red), and neuronal markers (white) (Fig. 4B, 4C, and S4C–S4E). The adenosine receptor $A_{2A}R$ was used as a marker for i-MSNs instead of D_2R, because of its exclusive somatodendritic expression (22). The location of dopamine synapses was identified by the presence of NL2 clusters apposing TH-positive dopaminergic terminals on GFP-labeled dendrites (Fig. 4A). These

NL2-clustered dopamine synapses were richly expressed on spiny dendrites of both D_1R-positive d-MSNs and A_{2A}R-positive i-MSNs (Fig. 4B and 4C; arrows), whereas they were rare on aspiny dendrites of GABAergic and cholinergic interneurons labeled for PV, nNOS, and CHT (Fig. S4C–S4E). Instead, most NL2 clusters on these interneuron dendrites were judged to be non-dopamine synapses, as they did not appose TH-positive dopaminergic terminals (Fig. S4C–S4E; arrowheads).

We measured the density of NL2-clustered dopamine and non-dopamine synapses on MSNs. The density of dopamine synapses on dendritic shafts (0.75-1.5 μm diameter) in d-MSNs and i-MSNs was significantly (3–4-fold) higher than that in interneurons (Fig. 4D, open columns), whereas that of non-dopamine synapses showed no significant differences among striatal neurons (Fig. 4E). The density of dopamine synapses on dendritic spines was also comparable between the two types of MSNs (Fig. 4D, filled columns). Therefore, dendrites of d-MSNs and i-MSNs are targeted equally as a substrate for dopamine synapse formation.

NL2-mediated presynaptic differentiation in vitro

We hypothesized that GABAergic postsynaptic molecules mediated dopamine synapse formation, as they do for GABAergic synapse formation (21). To pursue this possibility, we co-cultured primary midbrain or striatal neurons at 9–11 days *in vitro* with HEK293T cells expressing $GABA_AR\alpha1$, NL2, or GFP, and examined whether presynaptic molecules were recruited to their contact sites (Fig. 5A and S5A). In this co-culture assay, CAST, VMAT2, and Nrxn were robustly and significantly recruited to contact sites between DAT-labeled dopaminergic axons and HEK293T cells expressing NL2 (Fig. 5B, 5E–5G), but not $GABA_AR\alpha1$ or GFP (Fig. 5C and 5D). Similar

presynaptic differentiation was observed in co-cultures of striatal GABAergic neurons with HEK293T cells expressing NL2 (Fig. S5B–S5E). Therefore, NL2 induces presynaptic differentiation in axons of midbrain dopamine neurons and striatal GABAergic neurons *in vitro*.

NL3 upregulates at dopamine synapses in NL2-knockout mice

To explore this role *in vivo*, changes in the density of dopamine synapses and molecular expression were investigated in NL2-knockout (KO) mice. We assessed the density of DAT-labeled dopamine synapses by measuring their nearest-neighbor distances. No significant differences in dopamine synapse density were found between wild-type and NL2-KO mice (Fig. S5G–S5I). Immunofluorescence and immunogold labelings for presynaptic VMAT2 (Fig. S5J–S5N) and postsynaptic gephyrin (Fig. S5O–S5S) were comparable at TH-labeled dopamine synapses between wild-type and NL2-KO mice, while significant upregulation of NL3 occurred at dopamine synapses in NL2-KO mice (Fig. S5T–S5X). In co-cultures with HEK293T cells expressing NL3, NL3 also induced presynaptic differentiation in dopaminergic axons *in vitro* (Fig. S5F). Therefore, we concluded that the role of NL2 in dopamine synapse formation *in vivo* could not be addressed using NL2-KO mice, owing to compensatory upregulation of NL3.

Reciprocal changes of dopamine and GABAergic synapses by NL2 knockdown

To overcome this problem, we employed a sparse knockdown (KD) of NL2, which has been used to uncover the role of NL1 in cortical synaptogenesis (23). We prepared control-microRNA (miR), NL2-miR#1, and NL2-miR#2. Both NL2-miRs effectively and selectively reduced NL2 expression in HEK293T cells (Fig. S6A). We injected

lentivirus vectors carrying GFP and one of the three miRs into the striatum of newborn pups (Fig. S6B). Two months after injection, a few MSNs expressed GFP (Fig. S6C; 12 of 765 DARPP32-positive MSNs). We first checked NL2 expression at gephyrin clusters on GFP-labeled spiny dendrites. No significant changes were observed in the density or fluorescent intensity of gephyrin clusters between control-miR-infected (control) and NL2-miR-infected (NL2-KD) neurons (Fig. S6D–S6F, red; Fig. S6G and S6H). At gephyrin clusters, fluorescent intensity for NL2 was markedly and significantly lower in NL2-KD neurons (Fig. S6D–S6F, white arrowheads; Fig. S6I), but not in neighboring non-infected neurons (Fig. S6D–S6F, yellow arrowheads). Notably, the fluorescence intensity for NL3 at gephyrin clusters showed no significant differences between control and NL2-KD neurons (Fig. S6J–S6L, white arrowheads; Fig. S6M). Therefore, injection of NL2-miRs effectively reduces NL2 expression in MSNs without affecting the total number and intensity of gephyrin clusters or NL3 expression at gephyrin clusters.

Next, we analyzed the density of dopamine and GABAergic synapses by counting the number of gephyrin clusters on GFP-labeled spiny dendrites that apposed TH-positive dopaminergic terminals (Fig. 6A–6C, arrows) or VIAAT-positive GABAergic terminals (arrowheads), respectively. In NL2-KD neurons, the density of dopamine synapses was significantly lower than in control neurons (Fig. 6D), whereas that of GABAergic synapses was significantly greater (Fig. 6E).

Discussion

In the present study, we have shown that striatal dopamine synapses are neurochemically-mismatched contacts, and NL2 is involved in their formation.

Neurochemically-mismatched contact at dopamine synapses

Dopaminergic terminals were extensively co-labeled for TH, DAT, and VMAT2, which are essential for the synthesis, recycling, and vesicular filling of dopamine (24). Moreover, CAST and Nrxn, which are involved in active zone formation and synaptic adhesion, respectively (6, 25), accumulated on the presynaptic membrane at dopamine synapses and were expressed at levels comparable to conventional glutamatergic and GABAergic synapses. This orchestrated molecular architecture consolidates the dopaminergic phenotype in the presynaptic side of dopamine synapses. Surprisingly, GABAergic proteins $GABA_AR\alpha1$, gephyrin, and NL2 were expressed in the postsynaptic side at densities comparable to those at conventional GABAergic synapses. Therefore, dopamine synapses are contacts between dopaminergic presynaptic and GABAergic postsynaptic structures. It has been reported that 40.7% of symmetric synapses expressing $GABA_A$ receptors in the striatum are formed by terminals in which GABA is low or undetectable (26). We assume that they represent mostly, if not all, dopamine synapses.

An increasing number of reports is emerging of cases in which two or more classical transmitters are co-released at single synapses (27), and dopamine has been shown to be co-released with glutamate or GABA (27, 28). However, we found no significant immunoreactivity for GABA, GAD, or VIAAT at dopaminergic terminals. The scarcity of GABA in dopaminergic terminals is consistent with previous studies reporting that no or few (11–13%) dopaminergic terminals are significantly labeled for GABA (18, 29). This suggests that GABA is co-released little, if any, at most dopamine synapses. Nevertheless, optogenetic stimulation of dopaminergic axons evokes $GABA_A$

receptor-mediated postsynaptic currents in MSNs through GAT1-mediated uptake and VMAT2-dependent vesicular filling of GABA (28, 30). In the present study, we observed weak expression of GAT1 as well as intense expression of VMAT2 in dopaminergic terminals. Together, this evidence indicates that the phenotypes of the major transmitters and receptors are neurochemically mismatched at dopamine synapses, but transporter-mediated GABA release could be conducted from dopaminergic terminals whose GABA content is undetectable by conventional immunohistochemistry or from a small subpopulation of dopaminergic terminals expressing high content of GABA.

NL-mediated dopamine synapse formation

Synapse type-specific transsynaptic interaction between NLs and Nrxns plays a key role in bi-directional synaptic differentiation (6). NL2 is selectively expressed at inhibitory synapses (8), binds gephyrin, and promotes its membrane targeting through collybistin activation (31). NL2 also interacts with $GABA_A$ receptors (20). These interactions underlie NL2-mediated specification of inhibitory synapses (9). Expression of NL2 at dopamine synapses, together with that of $GABA_AR\alpha1$ and gephyrin, is thus consistent with the framework of synapse type-dependent expression of the NL family. Our finding that significant amounts of CAST, VMAT2, and Nrxn were recruited to contact sites between dopaminergic axons and NL2-expressing HEK293T cells indicates that NL2 functions as a presynaptic organizer for dopaminergic axons *in vitro*, similarly to GABAergic axons (20, 32).

In vitro experiments clearly demonstrate that manipulations that up- or downregulate NL expression alter synapse formation positively or negatively,

respectively, indicating that NLs are intrinsically synaptogenic (9, 33). However, there is little or no change in the number and structure of synapses between global NL-KO and wild-type mice (23, 34). Indeed, we found no significant changes in the density of dopamine synapses in the striatum of NL2-KO mice. These conflicting results between the *in vitro* and *in vivo* conditions seem to be ascribed to the redundancy in the molecular form of NLs and Nrxns and their interactions (6). In support of this notion, NL3 was upregulated at dopamine synapses in NL2-KO mice, which would mask synaptogenic actions by NL2. To overcome this problem, we adopted the sparse NL2-KD strategy to minimize compensatory upregulation of NL3. Under this condition, the density of dopamine and GABAergic synapses on MSN dendrites was significantly decreased, and increased, respectively, without a change in their total density. This suggests that NL2 mediates striatal synapse formation by giving competitive advantage to heterologous dopamine synapses over conventional GABAergic synapses. Therefore, NL2 appears to regulate the formation of striatal synapses in a competitive and input-dependent manner *in vivo* rather than in a simple synaptogenic manner *in vitro*. Such NL-dependent competitive synaptogenesis has also been reported for NL1 in the cortex, where cortical synapse formation is sensitive to sparse NL1-KD causing transcellular differences in the relative amount of NL1 (23). Thus, different relative amounts of NL2 caused by sparse KD may also affect competitive synaptogenic processes between NL2-KD and control MSNs.

Postulated role of dopamine synapses

D_1R and D_2R are widely expressed on the extrasynaptic surface of MSN dendrites (15-17). The present immunohistochemistry confirmed this, and further clarified the

lack of dopamine receptor accumulation at dopamine synapses. The mismatching between dopamine release and reception sites indicates that dopamine synapses are neither the neural device for the *wired* transmission that is conducted for fast and point-to-point signaling typical to conventional glutamatergic and GABAergic synapses, nor that for the *volume* transmission for slow and global modulation, such as muscarinic M1-mediated cholinergic transmission in the hippocampus (35, 36). Then, what is the role of neurochemical-mismatched dopamine synapses?

Glutamatergic transmission to MSNs by cortical and thalamic inputs, and its modulation by dopaminergic, cholinergic, and GABAergic inputs, are the basis of functional regulation in the basal ganglia (10, 14). The diffusion model of quantal dopamine release postulates an effective radius of ~2 and 7 μm for the activation of D_1R and D_2R, respectively (37). A recent study using a D_2R biosensor points out that the spatiotemporal extent of dopaminergic transmission is more limited and D_2R on MSNs functionally behaves as low-affinity receptors for fast dopaminergic transmission (38). Considering that MSN dendrites are both the preferential postsynaptic target of dopamine synapse formation and the neuronal element enriched with dopamine receptors, we suggest that such heterologous contacts function as a device to increase the target specificity and potency of dopaminergic modulation by anchoring dopamine release sites to dopamine-sensing neurons. In this regard, it should be noted that synaptic contacts are also formed by other neuromodulatory neurons (39-41). Of these, NL2 is expressed at symmetric synapses formed by cholinergic neurons in the forebrain (42). The possibility that NL2-dependent formation of neurochemically-mismatched contacts could be the general strategy to attract neuromodulatory inputs to specific targets is an intriguing issue to be explored in future studies.

Materials and Methods

In the present study, we performed immunoblot, immunohistochemistry, lentiviral experiments, and co-culture assay. More information about the experimental procedures and the combination and specificity of antibodies is available in the Supporting Information.

Acknowledgments

This study was supported by Grants-in-Aid for Scientific Research (24220007 to MW; 15K06732 to MU). We thank Dr. Kensuke Futai at the University of Massachusetts Medical School for his kind gift of plasmid vectors encoding Nrxn1α–3α cDNA, and St. Jude Children's Research Hospital for providing the lentiviral vector system.

References

1. Gray EG (1959) Axo-somatic and axo-dendritic synapses of the cerebral cortex: an electron microscope study. *J Anat* 93:420-433.
2. Kuzirian MS & Paradis S (2011) Emerging themes in GABAergic synapse development. *Prog Neurobiol* 95(1):68-87.
3. Lardi-Studler B & Fritschy JM (2007) Matching of pre- and postsynaptic specializations during synaptogenesis. *The Neuroscientist : a review journal bringing neurobiology, neurology and psychiatry* 13(2):115-126.
4. Spitzer NC & Borodinsky LN (2008) Implications of activity-dependent neurotransmitter-receptor matching. *Philosophical transactions of the Royal Society of London. Series B, Biological sciences* 363(1495):1393-1399.
5. Williams ME, de Wit J, & Ghosh A (2010) Molecular mechanisms of synaptic specificity in developing neural circuits. *Neuron* 68(1):9-18.
6. Sudhof TC (2008) Neuroligins and neurexins link synaptic function to cognitive disease. *Nature* 455(7215):903-911.
7. Song JY, Ichtchenko K, Sudhof TC, & Brose N (1999) Neuroligin 1 is a postsynaptic cell-adhesion molecule of excitatory synapses. *Proc Natl Acad Sci U S A* 96(3):1100-1105.
8. Varoqueaux F, Jamain S, & Brose N (2004) Neuroligin 2 is exclusively localized to inhibitory synapses. *Eur J Cell Biol* 83(9):449-456.
9. Chubykin AA, *et al.* (2007) Activity-dependent validation of excitatory versus inhibitory synapses by neuroligin-1 versus neuroligin-2. *Neuron* 54(6):919-931.
10. Gerfen CR & Surmeier DJ (2011) Modulation of striatal projection systems by dopamine. *Annual review of neuroscience* 34:441-466.
11. Schultz W (2007) Multiple dopamine functions at different time courses. *Annual review of neuroscience* 30:259-288.
12. Freund TF, Powell JF, & Smith AD (1984) Tyrosine hydroxylase-immunoreactive boutons in synaptic contact with identified striatonigral neurons, with particular reference to dendritic spines. *Neuroscience* 13(4):1189-1215.
13. Pickel VM, Beckley SC, Joh TH, & Reis DJ (1981) Ultrastructural immunocytochemical localization of tyrosine hydroxylase in the neostriatum. *Brain Res* 225(2):373-385.
14. Moss J & Bolam JP (2008) A dopaminergic axon lattice in the striatum and its relationship with cortical and thalamic terminals. *J Neurosci* 28(44):11221-11230.

15. Caille I, Dumartin B, & Bloch B (1996) Ultrastructural localization of D1 dopamine receptor immunoreactivity in rat striatonigral neurons and its relation with dopaminergic innervation. *Brain Res* 730(1-2):17-31.
16. Sesack SR, Aoki C, & Pickel VM (1994) Ultrastructural localization of D2 receptor-like immunoreactivity in midbrain dopamine neurons and their striatal targets. *J Neurosci* 14(1):88-106.
17. Yung KK, *et al.* (1995) Immunocytochemical localization of D1 and D2 dopamine receptors in the basal ganglia of the rat: light and electron microscopy. *Neuroscience* 65(3):709-730.
18. Stensrud MJ, Puchades M, & Gundersen V (2013) GABA is localized in dopaminergic synaptic vesicles in the rodent striatum. *Brain Struct Funct*.
19. Arluison M & Delamanche IS (1980) High-Resolution Autoradiographic Study of the Serotonin Innervation of the Rat Corpus Striatum after Intraventricular Administration of [H-3]5-Hydroxytryptamine. *Neuroscience* 5(2):229-+.
20. Dong N, Qi J, & Chen G (2007) Molecular reconstitution of functional GABAergic synapses with expression of neuroligin-2 and GABAA receptors. *Mol Cell Neurosci* 35(1):14-23.
21. Tyagarajan SK & Fritschy JM (2014) Gephyrin: a master regulator of neuronal function? *Nature reviews. Neuroscience* 15(3):141-156.
22. Quiroz C, *et al.* (2009) Key modulatory role of presynaptic adenosine A2A receptors in cortical neurotransmission to the striatal direct pathway. *TheScientificWorldJournal* 9:1321-1344.
23. Kwon HB, *et al.* (2012) Neuroligin-1-dependent competition regulates cortical synaptogenesis and synapse number. *Nat Neurosci* 15(12):1667-1674.
24. Pereira DB & Sulzer D (2012) Mechanisms of dopamine quantal size regulation. *Frontiers in bioscience* 17:2740-2767.
25. Ohtsuka T (2013) CAST: functional scaffold for the integrity of the presynaptic active zone. *Neuroscience research* 76(1-2):10-15.
26. Fujiyama F, Fritschy JM, Stephenson FA, & Bolam JP (2000) Synaptic localization of GABA(A) receptor subunits in the striatum of the rat. *J Comp Neurol* 416(2):158-172.
27. El Mestikawy S, Wallen-Mackenzie A, Fortin GM, Descarries L, & Trudeau LE (2011) From glutamate co-release to vesicular synergy: vesicular glutamate transporters. *Nature reviews. Neuroscience* 12(4):204-216.
28. Tritsch NX, Ding JB, & Sabatini BL (2012) Dopaminergic neurons inhibit striatal output through non-canonical release of GABA. *Nature*

490(7419):262-266.

29. Hanley JJ & Bolam JP (1997) Synaptology of the nigrostriatal projection in relation to the compartmental organization of the neostriatum in the rat. *Neuroscience* 81(2):353-370.
30. Tritsch NX, Oh WJ, Gu C, & Sabatini BL (2014) Midbrain dopamine neurons sustain inhibitory transmission using plasma membrane uptake of GABA, not synthesis. *eLife* 3:e01936.
31. Poulopoulos A, *et al.* (2009) Neuroligin 2 drives postsynaptic assembly at perisomatic inhibitory synapses through gephyrin and collybistin. *Neuron* 63(5):628-642.
32. Scheiffele P, Fan J, Choih J, Fetter R, & Serafini T (2000) Neuroligin expressed in nonneuronal cells triggers presynaptic development in contacting axons. *Cell* 101(6):657-669.
33. Chih B, Engelman H, & Scheiffele P (2005) Control of excitatory and inhibitory synapse formation by neuroligins. *Science* 307(5713):1324-1328.
34. Varoqueaux F, *et al.* (2006) Neuroligins determine synapse maturation and function. *Neuron* 51(6):741-754.
35. Agnati LF, Guidolin D, Guescini M, Genedani S, & Fuxe K (2010) Understanding wiring and volume transmission. *Brain research reviews* 64(1):137-159.
36. Yamasaki M, Matsui M, & Watanabe M (2010) Preferential localization of muscarinic M1 receptor on dendritic shaft and spine of cortical pyramidal cells and its anatomical evidence for volume transmission. *J Neurosci* 30(12):4408-4418.
37. Rice ME, Patel JC, & Cragg SJ (2011) Dopamine release in the basal ganglia. *Neuroscience* 198:112-137.
38. Marcott PF, Mamaligas AA, & Ford CP (2014) Phasic dopamine release drives rapid activation of striatal D2-receptors. *Neuron* 84(1):164-176.
39. Seguela P, Watkins KC, & Descarries L (1989) Ultrastructural relationships of serotonin axon terminals in the cerebral cortex of the adult rat. *J Comp Neurol* 289(1):129-142.
40. Seguela P, Watkins KC, Geffard M, & Descarries L (1990) Noradrenaline axon terminals in adult rat neocortex: an immunocytochemical analysis in serial thin sections. *Neuroscience* 35(2):249-264.
41. Wainer BH, *et al.* (1984) Cholinergic synapses in the rat brain: a correlated light and electron microscopic immunohistochemical study employing a monoclonal

antibody against choline acetyltransferase. *Brain Res* 308(1):69-76.

42. Takacs VT, Freund TF, & Nyiri G (2013) Neuroligin 2 is expressed in synapses established by cholinergic cells in the mouse brain. *PLoS One* 8(9):e72450.
43. tom Dieck S, *et al.* (2012) Deletion of the presynaptic scaffold CAST reduces active zone size in rod photoreceptors and impairs visual processing. *J Neurosci* 32(35):12192-12203.
44. Fukabori R, *et al.* (2012) Striatal direct pathway modulates response time in execution of visual discrimination. *Eur J Neurosci* 35(5):784-797.
45. Sano H, *et al.* (2003) Conditional ablation of striatal neuronal types containing dopamine D2 receptor disturbs coordination of basal ganglia function. *J Neurosci* 23(27):9078-9088.
46. Fukaya M, *et al.* (2006) Abundant distribution of TARP gamma-8 in synaptic and extrasynaptic surface of hippocampal neurons and its major role in AMPA receptor expression on spines and dendrites. *Eur J Neurosci* 24(8):2177-2190.
47. Uchigashima M, *et al.* (2007) Subcellular arrangement of molecules for 2-arachidonoyl-glycerol-mediated retrograde signaling and its physiological contribution to synaptic modulation in the striatum. *J Neurosci* 27(14):3663-3676.
48. Yamasaki M, *et al.* (2014) Opposing role of NMDA receptor GluN2B and GluN2D in somatosensory development and maturation. *J Neurosci* 34(35):11534-11548.
49. Iwakura A, Uchigashima M, Miyazaki T, Yamasaki M, & Watanabe M (2012) Lack of molecular-anatomical evidence for GABAergic influence on axon initial segment of cerebellar Purkinje cells by the pinceau formation. *J Neurosci* 32(27):9438-9448.
50. Miura E, *et al.* (2006) Expression and distribution of JNK/SAPK-associated scaffold protein JSAP1 in developing and adult mouse brain. *J Neurochem* 97(5):1431-1446.
51. Fukaya M & Watanabe M (2000) Improved immunohistochemical detection of postsynaptically located PSD-95/SAP90 protein family by protease section pretreatment: a study in the adult mouse brain. *J Comp Neurol* 426(4):572-586.
52. Somogyi J, *et al.* (2004) GABAergic basket cells expressing cholecystokinin contain vesicular glutamate transporter type 3 (VGLUT3) in their synaptic terminals in hippocampus and isocortex of the rat. *Eur J Neurosci* 19(3):552-569.

Figure Legends

Fig. 1 Dopaminergic presynaptic phenotype at striatal dopamine synapses. (*A* and *B*) Immunofluorescence labeling for TH (*A*) and DAT (*B*) in the striatum. Cx, cortex; NA, nucleus accumbens; St, striatum. (*C*) Triple immunofluorescence for TH (red), DAT (green), and VMAT2 (blue) in ultrathin (100 nm) cryosections showing their extensive overlap (arrows). (*D* and *E*) Double-label post-embedding immunoelectron microscopy for GABA (Ø = 10-nm colloidal gold particles) and VIAAT (*D*; Ø = 15 nm) or TH (*E*; Ø = 15 nm). GABA (arrows) is concentrated on VIAAT-positive GABAergic terminals forming symmetric synapses (NT-GABA; red terminal), but not detected in VIAAT-negative glutamatergic terminals forming asymmetric synapses (NT-Glu; blue) or TH-positive dopaminergic terminals (NT-DA; green) forming symmetric synapses. Arrowhead pairs indicate the synaptic membrane. Dn, dendrite; NT, nerve terminal; Sp, spine. (*F*) The density of immunogold labeling for GABA (particles per 1 μm^2) in dopaminergic (DA), GABAergic (GABA), and glutamatergic (Glu) terminals. (*G* and *I*) Double-label post-embedding immunogold microscopy for TH (Ø = 15 nm) and CAST (*G*; Ø = 10 nm) or Nrxn (*I*; Ø = 10 nm). Immunogold labeling (arrows) for CAST and Nrxn is observed beneath the presynaptic membrane of TH-positive dopaminergic terminals. (*H* and *J*) The mean density of immunogold particles per 1 μm of synaptic membrane for CAST (*H*) and Nrxn (*J*) at dopaminergic, GABAergic, and glutamatergic synapses in wild-type (*H* and *J*; open columns) and CAST-knockout (KO) (*H*; filled columns) mice. In F, H, J, numbers of terminals analyzed are indicated above each column, and error bars on columns represent SEM. *$p < 0.05$ (unpaired *t* test). Scale bars: 1 mm (*A* and *B*), 2 μm (*C*), 100 nm (*D*, *E*, *G*, and *I*).

Fig. 2 Expression profiles of dopamine receptors in the striatum. (*A* and *B*) Pre-embedding immunoelectron microscopy for D_1R (*A*) and D_2R (*B*). D_1R- and D_2R-labeled spiny dendrites are colored red and green, respectively. (*C*) Labeling densities for D_1R (left) and D_2R (right) per 1 μm of the plasma membrane in somata (So), dendritic shafts (Dn), dendritic spines (Sp), and nerve terminals forming asymmetric (NT-asy) or symmetric (NT-sym) synapses. (*D* and *E*) Double-label pre-embedding immunoelectron microscopy for TH (DAB) and D_1R (*D*; particles) or D_2R (*E*; particles). Arrowhead pairs indicate dopamine synapses. (*F*) The synaptic (black), perisynaptic (dark gray), and extrasynaptic (light gray) membranes of dendrites around dopamine synapses. (*G*) Densities for D_1R (left; 18 synapses) and D_2R (right; 16 synapses) labelings per 1 μm of the synaptic, perisynaptic, and extrasynaptic membranes. The length of the plasma membrane (μm) and the number of metal particles analyzed are indicated in parentheses or above each column, respectively. Error bars represent SEM. $*p < 0.05$ and $**p < 0.01$ (unpaired *t* test). Scale bars: 200 nm.

Fig. 3 GABAergic postsynaptic phenotype at striatal dopamine synapses. (*A–C*) Triple immunofluorescence for DAT (green) and VIAAT (blue), and for $GABA_AR\alpha1$ (*A*; red), gephyrin (*B*; red), or NL2 (*C*; red). Note close apposition of $GABA_AR\alpha1$, gephyrin, and NL2 clusters to both VIAAT-positive GABAergic terminals (arrowheads) and DAT-positive dopaminergic terminals (arrows). (*D–F*) Double-label post-embedding immunoelectron microscopy for TH (Ø = 15 nm) and for $GABA_AR\alpha1$ (*D*; Ø = 10-nm colloidal gold particles), gephyrin (*E*; Ø = 10 nm), or NL2 (*F*; Ø = 10 nm). Immunogold particles (arrows) are concentrated at symmetric synapses formed by

TH-labeled dopaminergic terminals (NT-TH, arrowhead pairs). (*G–I*) The density of immunogold labeling for $GABA_AR\alpha1$ (*G*), gephyrin (*H*), or NL2 (*I*) per 1 μm of synaptic membrane at dopamine (DA), GABAergic (GABA), and glutamatergic (Glu) synapses. The specificity of NL2 labeling is confirmed by almost blank labeling in NL2-knockout (KO) mice (*I*). Representative images of GABAergic synapses are shown in Fig. S3. Numbers of synapses analyzed are indicated above each column. Error bars represent SEM. *$p < 0.05$, **$p < 0.01$, and ***$p < 0.001$ (unpaired *t* test). Scale bars: 2 μm (*A–C*), 100 nm (*D–F*).

Fig. 4 Dopamine synapses are preferentially formed on to dendrites of two types of MSNs. (*A*) Schematic to distinguish NL2-clustered dopamine and non-dopamine synapses on GFP-labeled dendrites of striatal neurons. (*B* and *C*) Quadruple immunofluorescence for NL2 (red), GFP (green), and TH (blue), and for D_1R (*B*, white) or $A_{2A}R$ (*C*, white). NL2-clustered dopamine synapses (arrows) are preferentially distributed on dendrites of D_1R-labeled d-MSNs (*B*) and $A_{2A}R$-labeled i-MSNs (*C*). (*D* and *E*) The density of NL2-clustered dopamine (*D*) and non-dopamine (*E*) synapses per 10 μm of dendritic shafts (Dn) and spines (Sp) in d-MSNs and i-MSNs, and dendrites of striatal interneurons. Immunofluorescence images for striatal interneurons are shown in Fig. S4. The number of dendrites analyzed is indicated above each column. Error bars represent SEM. *$p < 0.05$ and ***$p < 0.001$ (one-way ANOVA with Tukey's *post hoc* test). Scale bars: 2 μm.

Fig. 5 NL2-mediated presynaptic differentiation of dopaminergic axons *in vitro*. (*A*) Schematic of co-culture assay of midbrain neurons with HEK293T cells expressing

NL2, $GABA_AR\alpha1$, or GFP. Axons of midbrain dopamine neurons were identified by DAT immunofluorescence. (*B–D*) Triple immunofluorescence for CAST (red) and DAT (green), and for NL2 (*B*; blue), $GABA_AR\alpha1$ (*C*; blue) or GFP (*D*; blue). CAST clusters are recruited to contact sites of dopaminergic axons with HEK293T cells expressing NL2 (*B*, arrowheads), but not $GABA_AR\alpha1$ (*C*) or GFP (*D*). (*E*) The density of CAST clusters per 100 μm of dopaminergic axon in contact with HEK293T cells. The number of HEK293T cells contacted by DAT-labeled dopaminergic axons is indicated above each column. Error bars represent SEM. ***$p < 0.001$ (Mann–Whitney U test). (*F* and *G*) Triple immunofluorescence for VMAT2 (*F*; red) or Nrxn (*G*; red), DAT (green), and NL2 (blue) in co-cultures of midbrain dopamine neurons and HEK293T cells expressing NL2. Scale bars: 2 μm.

Fig. 6 Decrease of dopamine synapses and reciprocal increase of GABAergic synapses after sparse NL2 knockdown in striatal MSNs. (*A–C*) Quadruple immunofluorescence for gephyrin (red), GFP (green), TH (blue), and VIAAT (gray) in spiny dendrites of control (*A*), NL2-knockdown (KD) #1 (*B*), or NL2-KD#2 (*C*) neurons. Arrows and arrowheads indicate dopamine and GABAergic synapses, respectively, on GFP-labeled dendrites. (*D* and *E*) The density of dopamine (*D*) and GABAergic (*E*) synapses per 10 μm of control and KD dendrites. The total number of dendrites analyzed is indicated above each column. Error bars represent SEM. *$p < 0.05$, **$p < 0.01$, and ***$p < 0.001$ (Mann–Whitney U test). Scale bars: 2 μm.

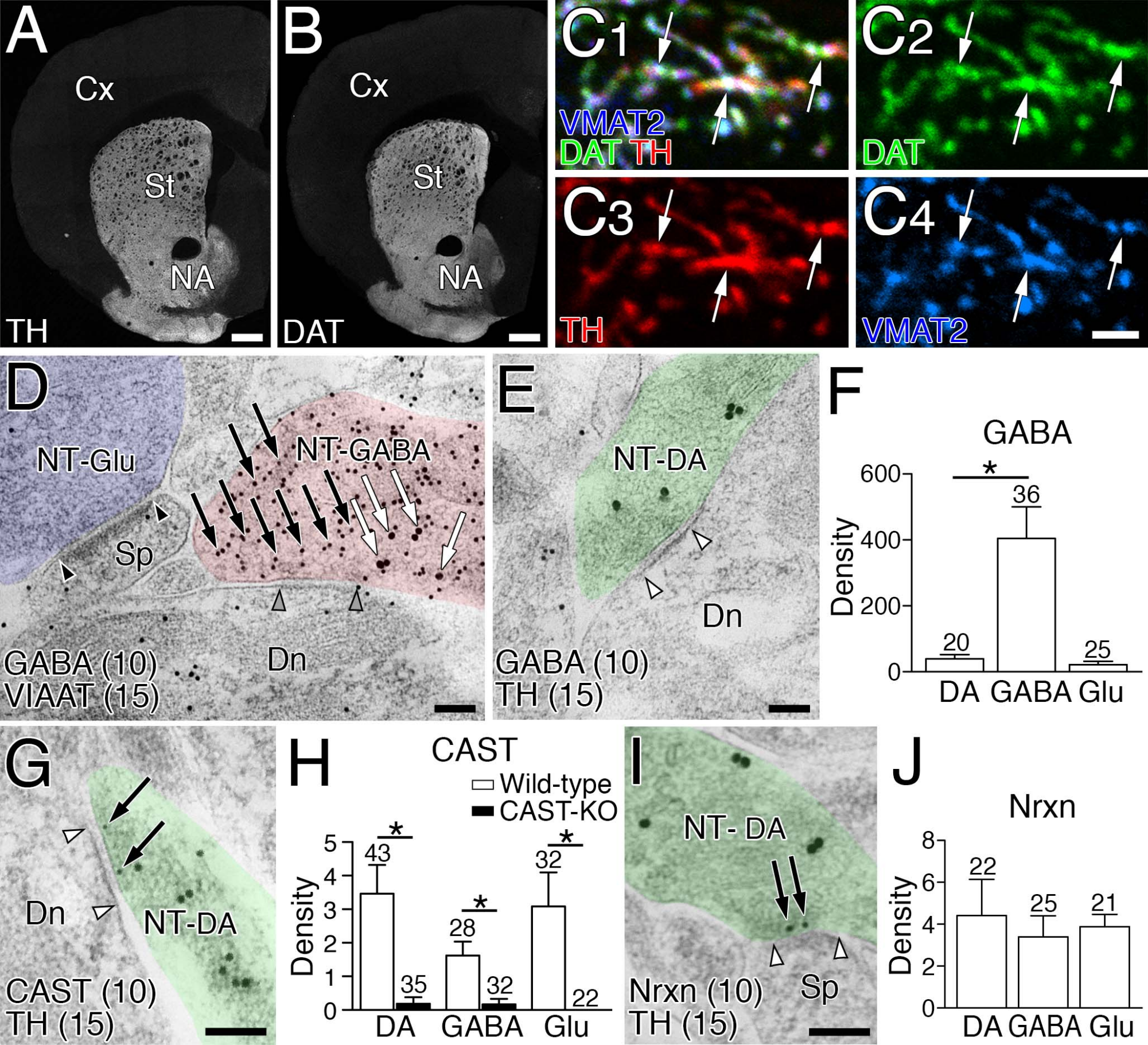
A
Cx
St
NA
TH
B
Cx
St
NA
DAT
C1
VMAT2
DAT TH
C2
DAT
C3
TH
C4
VMAT2
D
NT-Glu
NT-GABA
Sp
Dn
GABA (10)
VIAAT (15)
E
NT-DA
Dn
GABA (10)
TH (15)
F
GABA
Density
600
400
200
0
*
36
20
25
DA GABA Glu
G
Dn
NT-DA
CAST (10)
TH (15)
H
CAST
Wild-type
CAST-KO
Density
5
4
3
2
1
0
*
43
35
*
28
32
*
32
22
DA GABA Glu
I
NT- DA
Nrxn (10)
TH (15)
Sp
J
Nrxn
Density
8
6
4
2
0
22
25
21
DA GABA Glu

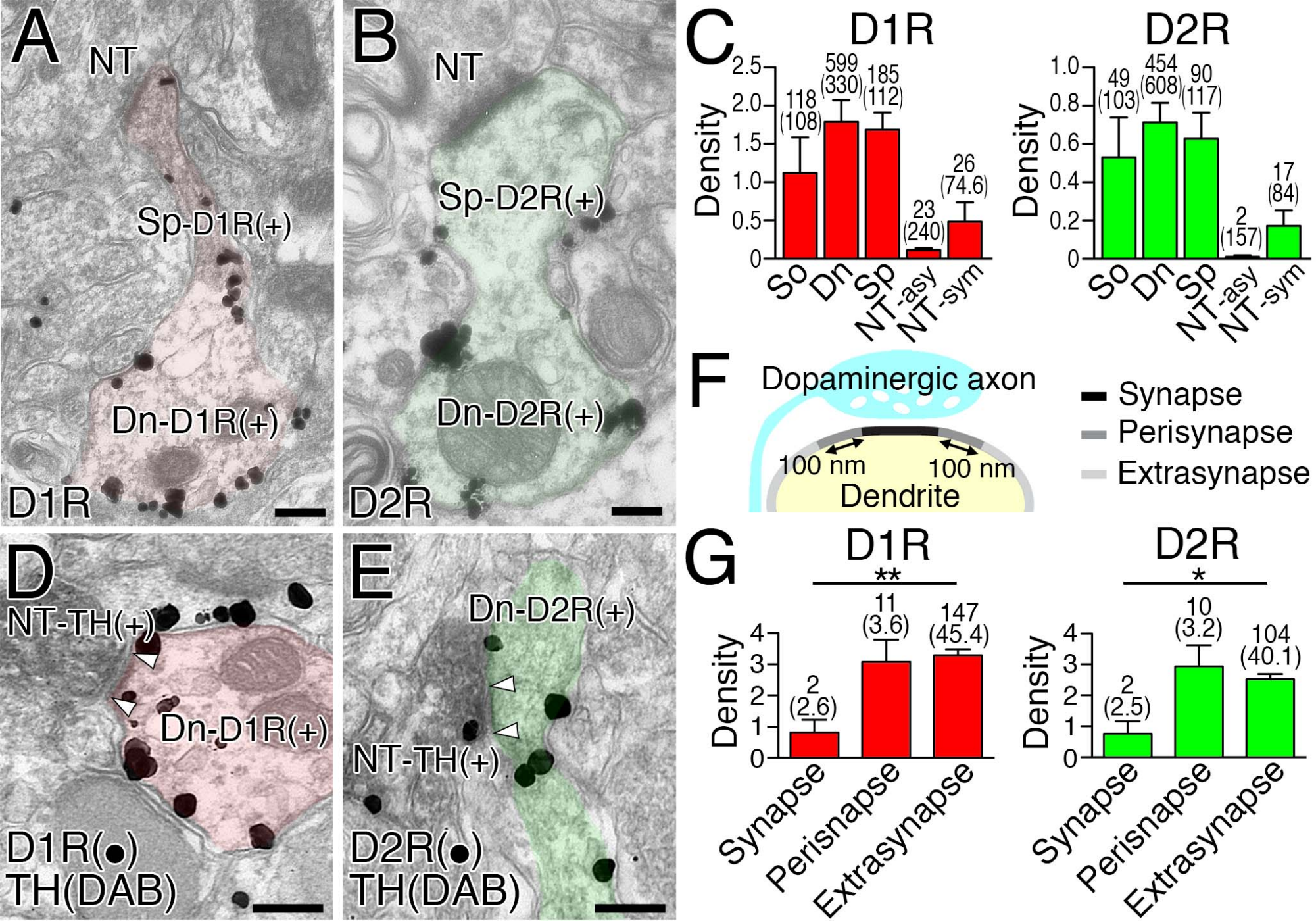
A
NT
Sp-D1R(+)
Dn-D1R(+)
D1R
B
NT
Sp-D2R(+)
Dn-D2R(+)
D2R
C
D1R
Density
118 (108)
599 (330)
185 (112)
23 (240)
26 (74.6)
So
Dn
Sp
NT-asy
NT-sym
D2R
49 (103)
454 (608)
90 (117)
2 (157)
17 (84)
D
NT-TH(+)
Dn-D1R(+)
D1R(●) TH(DAB)
E
Dn-D2R(+)
NT-TH(+)
D2R(●) TH(DAB)
F
Dopaminergic axon
100 nm
100 nm
Dendrite
Synapse
Perisynapse
Extrasynapse
G
D1R
**
2 (2.6)
11 (3.6)
147 (45.4)
Synapse
Perisnapse
Extrasynapse
D2R
*
2 (2.5)
10 (3.2)
104 (40.1)

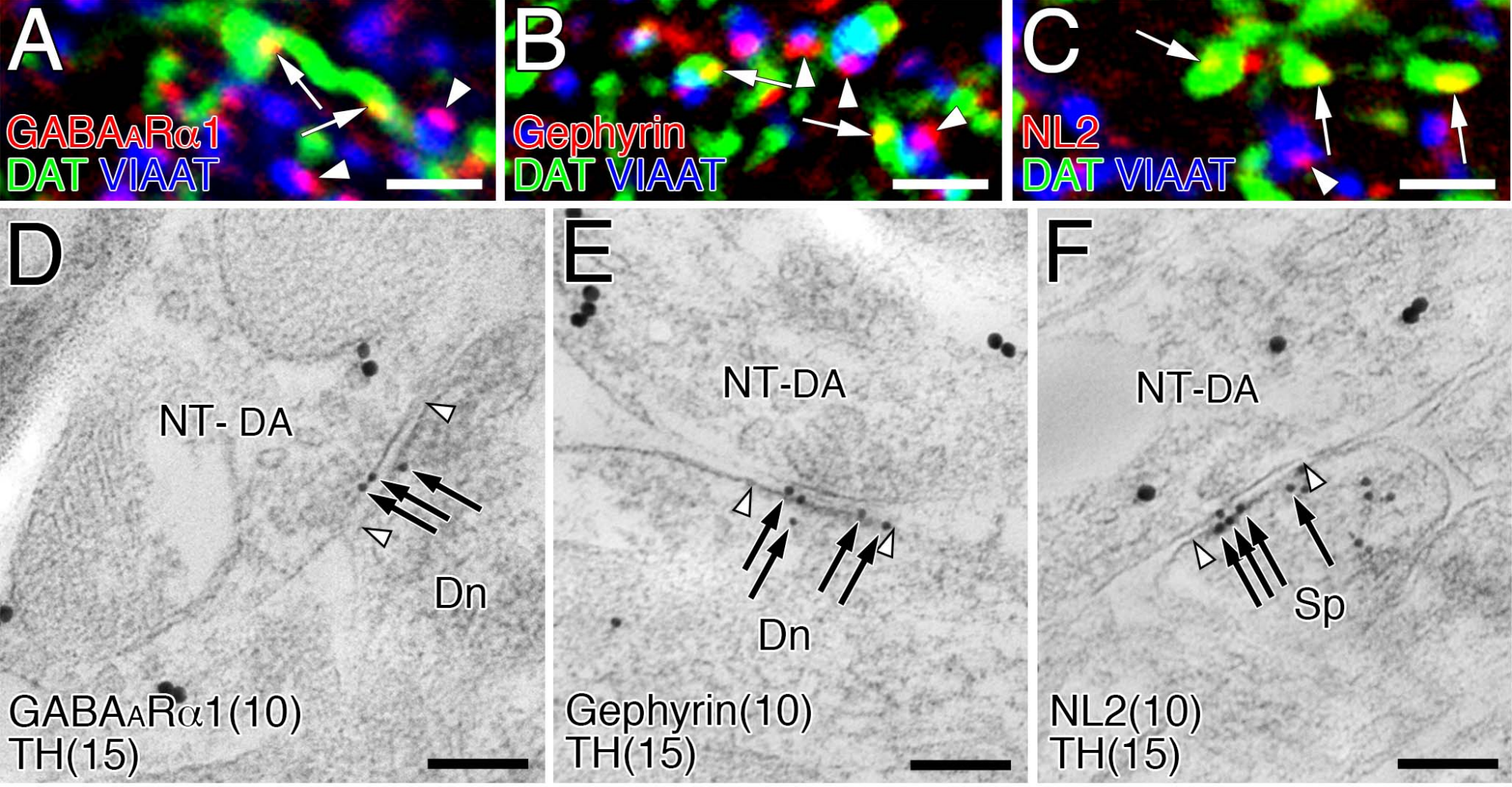
A
GABAARα1
DAT VIAAT
B
Gephyrin
DAT VIAAT
C
NL2
DAT VIAAT
D
NT- DA
Dn
GABAARα1(10)
TH(15)
E
NT-DA
Dn
Gephyrin(10)
TH(15)
F
NT-DA
Sp
NL2(10)
TH(15)

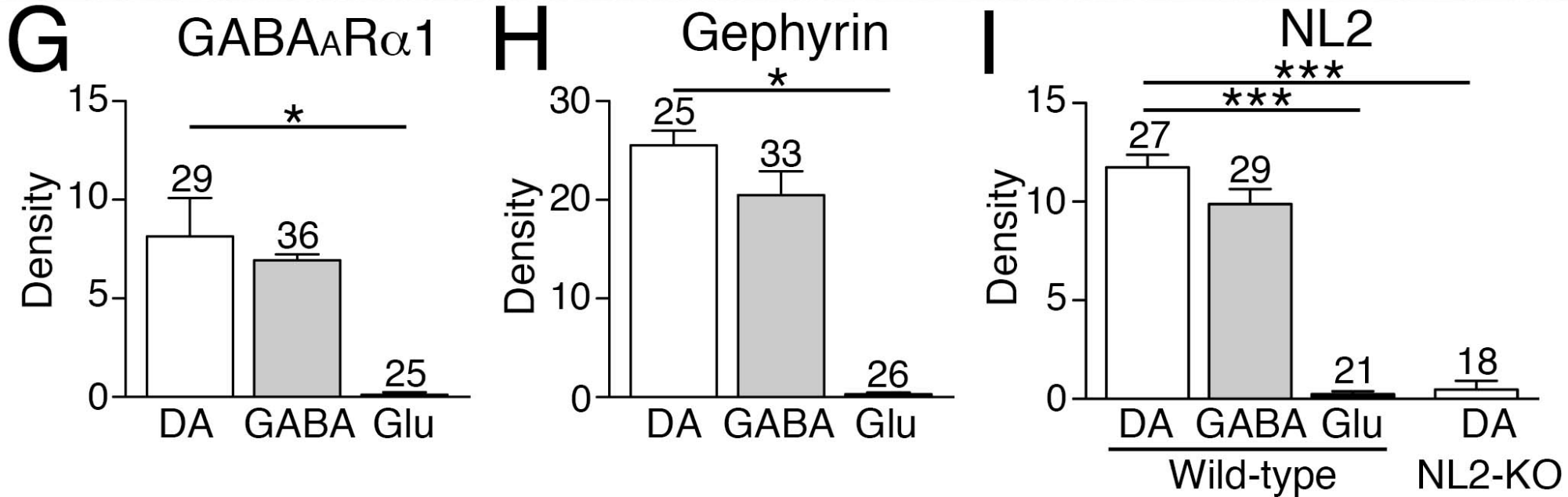
G
GABAARα1
Density
15
10
5
0
*
29
36
25
DA
GABA
Glu
H
Gephyrin
Density
30
20
10
0
*
25
33
26
DA
GABA
Glu
I
NL2
Density
15
10
5
0
***
***
27
29
21
18
DA
GABA
Glu
DA
Wild-type
NL2-KO

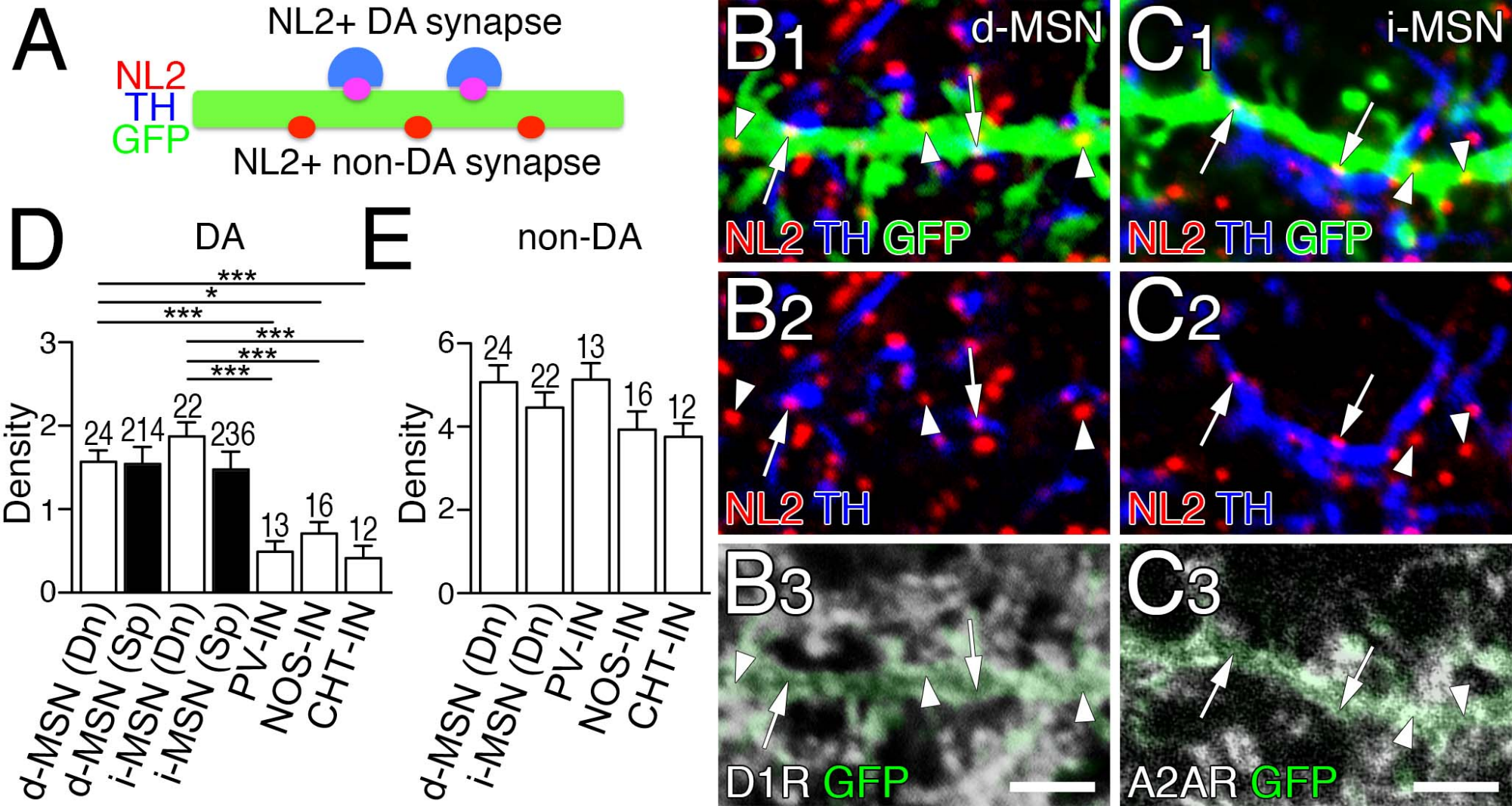
A
NL2+ DA synapse
NL2
TH
GFP
NL2+ non-DA synapse
B1
d-MSN
NL2 TH GFP
C1
i-MSN
NL2 TH GFP
B2
NL2 TH
C2
NL2 TH
B3
D1R GFP
C3
A2AR GFP
D
DA
***
*
***
***
***
***
Density
3
2
1
0
24
214
22
236
13
16
12
d-MSN (Dn)
d-MSN (Sp)
i-MSN (Dn)
i-MSN (Sp)
PV-IN
NOS-IN
CHT-IN
E
non-DA
Density
6
4
2
0
24
22
13
16
12
d-MSN (Dn)
i-MSN (Dn)
PV-IN
NOS-IN
CHT-IN

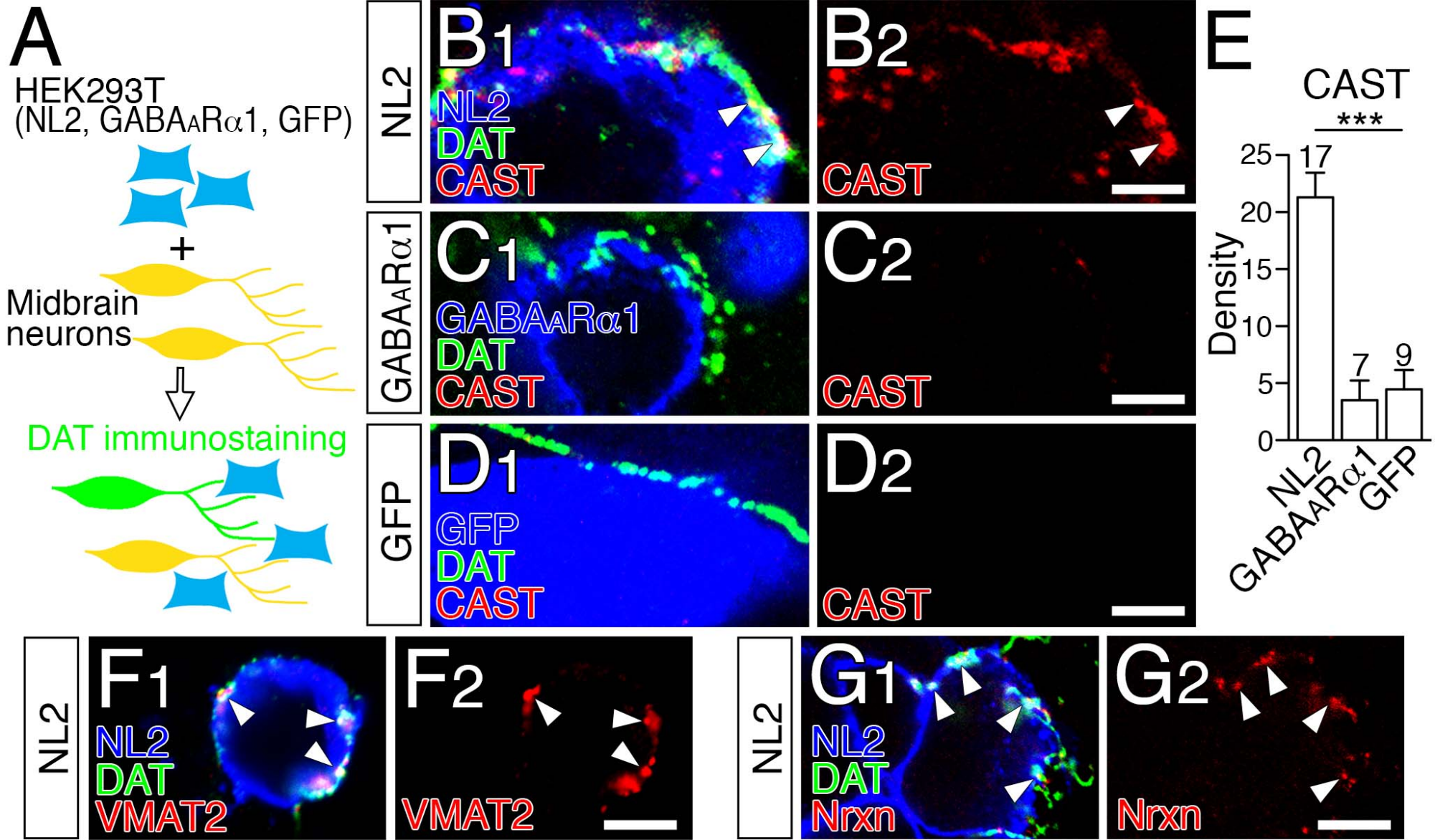
A
HEK293T
(NL2, GABAAα1, GFP)
+
Midbrain
neurons
DAT immunostaining
NL2
GABAAα1
GFP
B1
NL2
DAT
CAST
B2
CAST
C1
GABAAα1
DAT
CAST
C2
CAST
D1
GFP
DAT
CAST
D2
CAST
E
CAST
***
Density
25
20
15
10
5
0
17
7
9
NL2
GABAAα1
GFP
F1
NL2
DAT
VMAT2
F2
VMAT2
G1
NL2
DAT
Nrxn
G2
Nrxn

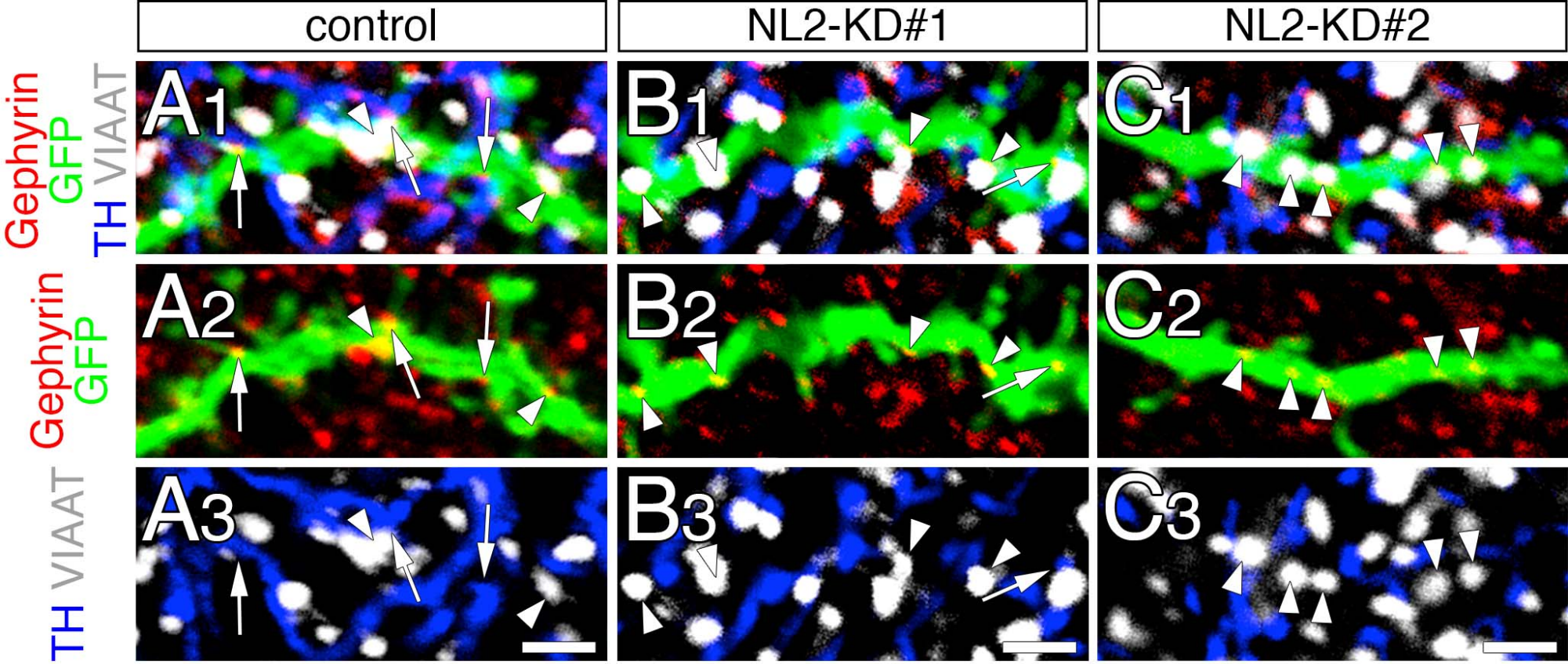
control
NL2-KD#1
NL2-KD#2
Gephyrin
GFP
TH VIAAT
A1
B1
C1
A2
B2
C2
A3
B3
C3

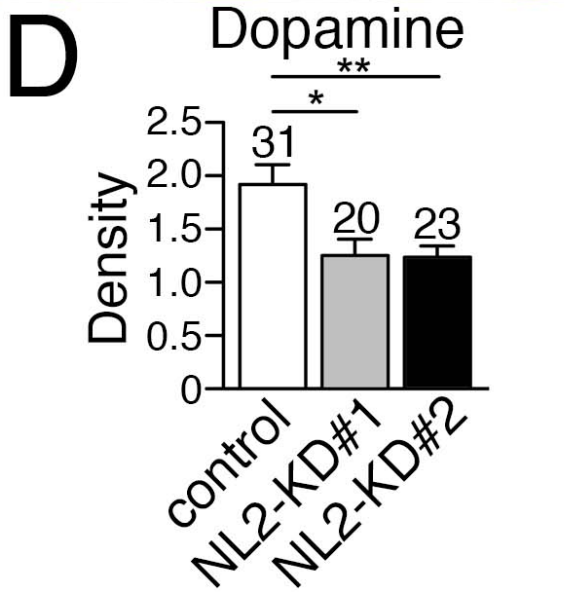
D
Dopamine
**
*
Density
2.5
2.0
1.5
1.0
0.5
0
31
20
23
control
NL2-KD#1
NL2-KD#2

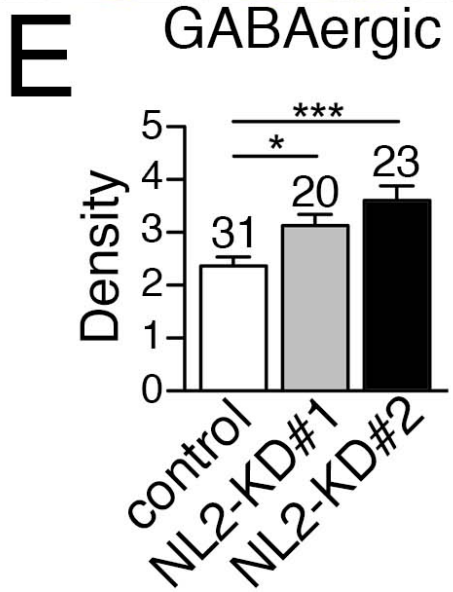
E
GABAergic
***
*
Density
5
4
3
2
1
0
31
20
23
control
NL2-KD#1
NL2-KD#2